

# Analytical approaches for large-scale structures in some modified-gravity scenarios

P. Valageas

IPhT - CEA Saclay

coll. with Ph. Brax

PRD, 86, 123501 (2012)  
PRD, 88, 023527 (2013)

arXiv:1403.5420  
1403.5424

# **Definition of the models**

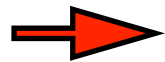
## a) f(R) models

Add a function of the Ricci scalar,  $f(R)$ , to the Einstein-Hilbert action:

$$S = \int d^4x \sqrt{-g} \left[ \frac{M_{\text{Pl}}^2}{2} (R + f(R)) + \mathcal{L}_m \right]$$

$$f(R) = -2\Lambda - \frac{f_{R_0} c^2}{n} \frac{R_0^{n+1}}{R^n} \quad n = 1, \quad |f_{R_0}| \leq 10^{-5}$$

Solar System constraints



Modified Poisson equation:

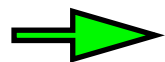
$$\nabla^2 \Psi = \frac{16\pi\mathcal{G}}{3} a^2 \delta\rho - \frac{a^2}{6} \delta R$$

Constraint equation:

$$\nabla^2 \delta f_R = \frac{a^2}{3} [\delta R - 8\pi\mathcal{G}\delta\rho]$$

$$f_R = \frac{df}{dR} = f_{R_0} c^2 \frac{R_0^{n+1}}{R^{n+1}}$$

Large scales



$$\nabla \rightarrow 0$$



we recover GR (in the weak field regime)

Nonlinear equation for  $\delta R(\delta\rho)$  but it is **self-averaging**:

$$\int_{\mathcal{V}} \frac{dV}{\mathcal{V}} \delta R = \frac{3}{a^2} \int_S \frac{dS}{\mathcal{V}} (\mathbf{n} \cdot \nabla \delta f_R) + 8\pi\mathcal{G} \frac{\delta M}{\mathcal{V}} \xrightarrow{\mathcal{V} \rightarrow \infty} 0$$

no cumulative contribution from small-scale nonlinearities: we recover the large-scale Hubble flow.

## b) Scalar field models

### I) Dilaton models

Scalar-tensor theories

$$S = \int d^4x \sqrt{-g} \left[ \frac{M_{\text{Pl}}^2}{2} R - \frac{1}{2} (\nabla\varphi)^2 - V(\varphi) \right] + \int d^4x \sqrt{-\tilde{g}} \mathcal{L}_m(\psi_m, \tilde{g}_{\mu\nu})$$

$$\tilde{g}_{\mu\nu} = A(\varphi)^2 g_{\mu\nu}$$

Jordan-frame metric

Einstein-frame metric



Modified Poisson equation (5th force):

$$\Psi = \Psi_N + \Psi_A$$

$$\nabla^2 \Psi_N = 4\pi \mathcal{G} a^2 \delta\rho$$

$$\Psi_A = c^2 (A - \bar{A}) \quad (A \simeq 1)$$

Klein-Gordon eq.: 
$$\frac{c^2}{a^2} \nabla^2 \varphi = \frac{dV}{d\varphi} + \rho \frac{dA}{d\varphi}$$

Small-scale nonlinearities are again **self-averaging** (e.g., periodic solutions).

## 2) K-mouflage models

$$S = \int d^4x \sqrt{-g} \left[ \frac{M_{\text{Pl}}^2}{2} R + \mathcal{L}_\varphi(\varphi) \right] + \int d^4x \sqrt{-\tilde{g}} \mathcal{L}_m(\psi_m^{(i)}, \tilde{g}_{\mu\nu})$$

Coupling matter -- scalar field through the Jordan metric conformal rescaling:  $\tilde{g}_{\mu\nu} = A^2(\varphi) g_{\mu\nu}$

Dilaton models, .. (chameleon screening):  $\mathcal{L}_\varphi = -(\partial\varphi)^2/2 - V(\varphi)$

Focus on **nonstandard kinetic term**:  $\mathcal{L}_\varphi(\varphi) = \mathcal{M}^4 K(\chi)$  with  $\chi = -\frac{1}{2\mathcal{M}^4} \partial^\mu \varphi \partial_\mu \varphi$

We recover a cosmological-constant behavior at late times in cases where:

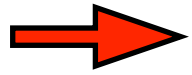
$$\chi \rightarrow 0 : \quad K(\chi) \simeq -1 + \chi + \dots \quad \mathcal{M}^4 = \rho_\Lambda$$

or if the first derivative of the kinetic function has a zero on the positive axis:

$$\chi_* > 0 : \quad K'(\chi_*) = 0, \quad K(\chi_*) < 0.$$

# **Perturbative approach**

1) Use the **quasi-static** approximation, which applies to small scales dominated by spatial gradients



Obtain a non-linear equation that relates the new field to the matter density

$$\mathcal{F}(\delta R, \delta\rho) = 0$$

$$\mathcal{F}(\delta\varphi, \delta\rho) = 0$$

This allows one to eventually go back to the standard LCDM formalism (i.e., we can **eliminate** the new degree of freedom).

2) Solve this equation through a perturbative **expansion over the nonlinear density** fluctuation

$$\delta\tilde{R}(\mathbf{k}) = \sum_{n=1}^{\infty} \int d\mathbf{k}_1 \dots d\mathbf{k}_n \delta_D(\mathbf{k}_1 + \dots + \mathbf{k}_n) h_n(\mathbf{k}_1, \dots, \mathbf{k}_n) \delta\tilde{\rho}(\mathbf{k}_1) \dots \delta\tilde{\rho}(\mathbf{k}_n)$$

$$\delta\tilde{\varphi}(\mathbf{k}) = \sum_{n=1}^{\infty} \int d\mathbf{k}_1 \dots d\mathbf{k}_n \delta_D(\mathbf{k}_1 + \dots + \mathbf{k}_n) h_n(\mathbf{k}_1, \dots, \mathbf{k}_n) \delta\tilde{\rho}(\mathbf{k}_1) \dots \delta\tilde{\rho}(\mathbf{k}_n)$$

3) Obtain the expression of the **full “gravitational” potential** (Newton+5th force)

$$\tilde{\Psi}(\mathbf{k}) = \sum_{n=1}^{\infty} \int d\mathbf{k}_1 \dots d\mathbf{k}_n \delta_D(\mathbf{k}_1 + \dots + \mathbf{k}_n) H_n(\mathbf{k}_1, \dots, \mathbf{k}_n) \delta\tilde{\rho}(\mathbf{k}_1) \dots \delta\tilde{\rho}(\mathbf{k}_n)$$

## a) f(R) models



Constraint equation:

$$\nabla^2 \delta f_R = \frac{a^2}{3} [\delta R - 8\pi \mathcal{G} \delta \rho]$$

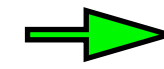
$$n \geq 1 : \quad \kappa_n(a) = H^{2n-2} \frac{d^n f_R}{dR^n}(\bar{R})$$

$$\left(1 - \frac{\nabla^2}{a^2 m^2}\right) \cdot \delta R = \frac{\delta \rho}{M_{\text{Pl}}^2} + \sum_{n=2}^{\infty} \frac{3H^{2-2n} \kappa_n}{a^2 n!} \nabla^2 (\delta R)^n$$



Modified Poisson equation:

$$\nabla^2 \Psi = \frac{16\pi \mathcal{G}}{3} a^2 \delta \rho - \frac{a^2}{6} \delta R$$



$$\Psi(\delta \rho)$$

## b) Scalar field models

### I) Dilaton models



Klein-Gordon eq.:

$$\frac{c^2}{a^2} \nabla^2 \varphi = \frac{dV}{d\varphi} + \rho \frac{dA}{d\varphi}$$

$$n \geq 1 : \quad \beta_n(a) = M_{\text{Pl}}^n \frac{d^n A}{d\varphi^n}(\bar{\varphi})$$

$$n \geq 2 : \quad \kappa_n(a) = \frac{M_{\text{Pl}}^{n-2}}{c^2} \left[ \frac{d^n V}{d\varphi^n}(\bar{\varphi}) + \bar{\rho} \frac{d^n A}{d\varphi^n}(\bar{\varphi}) \right]$$

$$\left(\frac{\nabla^2}{a^2} - m^2\right) \cdot \delta \varphi = \frac{\beta \delta \rho}{c^2 M_{\text{Pl}}} + \frac{\beta_2 \delta \rho}{c^2 M_{\text{Pl}}^2} \delta \varphi + \sum_{n=2}^{\infty} \left( \frac{\kappa_{n+1}}{M_{\text{Pl}}^{n-1}} + \frac{\beta_{n+1} \delta \rho}{c^2 M_{\text{Pl}}^{n+1}} \right) \frac{(\delta \varphi)^n}{n!}$$

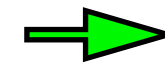


Modified Poisson equation (5th force):

$$\Psi = \Psi_N + \Psi_A$$

$$\Psi_A = c^2 (A - \bar{A})$$

$$\Psi_A = \sum_{n=1}^{\infty} \frac{c^2 \beta_n}{M_{\text{Pl}}^n n!} (\delta \varphi)^n$$



$$\Psi(\delta \rho)$$



## 2) K-mouflage models

★  $ctk/a \gg 1 : \quad \frac{1}{a^2} \nabla^2 \Psi_N = 4\pi \mathcal{G} \bar{A} \delta \rho$

★  $\frac{1}{a^3} \frac{\partial}{\partial t} \left( a^3 \frac{\partial \varphi}{\partial t} K' \right) - \frac{1}{a^2} \nabla \cdot (\nabla \varphi K') = -\frac{dA}{d\varphi} \rho \quad \Rightarrow \quad \frac{1}{a^2} \nabla \cdot (\nabla \delta \varphi K') = \frac{\bar{A} \beta_1}{M_{\text{Pl}}} \delta \rho$

$ctk/a \gg 1$       neglect time derivatives of the field fluctuations (while the background evolves with time and does not follow a quasi-static approximation).

4) Write the **equations of motion** (in the single-stream approximation), with the ``new gravitational potential''

Continuity eq.:  $\frac{\partial \delta}{\partial \tau} + \nabla \cdot [(1 + \delta)\mathbf{v}] = 0$

Euler eq.:  $\frac{\partial \mathbf{v}}{\partial \tau} + (\mathbf{v} \cdot \nabla)\mathbf{v} + \mathcal{H}\mathbf{v} = -\nabla\Psi$  (K-mouflage models)

$\frac{\partial \mathbf{v}}{\partial \tau} + (\mathbf{v} \cdot \nabla)\mathbf{v} + \left(\mathcal{H} + \frac{d \ln \bar{A}}{d\tau}\right)\mathbf{v} = -\nabla\Psi$

5th force
friction
5th force

This can be written in a more concise form as:

$$\mathcal{O}(x, x') \cdot \tilde{\psi}(x') = \sum_{n=2}^{\infty} K_n^s(x; x_1, \dots, x_n) \cdot \tilde{\psi}(x_1) \dots \tilde{\psi}(x_n)$$

2-component vector:  $\psi = \begin{pmatrix} \delta \\ -(\nabla \cdot \mathbf{v})/\dot{a} \end{pmatrix}$

time coordinate:  $\eta = \ln(a)$

$x = (\mathbf{k}, \eta, i)$

Linear part:  $\mathcal{O}(x, x') = \delta_D(\eta' - \eta) \delta_D(\mathbf{k}' - \mathbf{k}) \begin{pmatrix} \frac{\partial}{\partial \eta} & -1 \\ -\frac{3}{2}\Omega_m(1+\epsilon_1) & \frac{\partial}{\partial \eta} + \frac{1-3w_\varphi^{\text{eff}}\Omega_\varphi^{\text{eff}}}{2} + \epsilon_2 \end{pmatrix}$

modified-gravity impact at linear order

Equal-time kernels:  $K_n^s = \delta_D(\eta_1 - \eta) \dots \delta_D(\eta_n - \eta) \delta_D(\mathbf{k}_1 + \dots + \mathbf{k}_n) \gamma_{i; i_1, \dots, i_n}^s(\mathbf{k}_1, \dots, \mathbf{k}_n; \eta)$

## 5) Linear theory

★  $f(R)$  and dilaton models:

$$\frac{\partial^2 D}{\partial \eta^2} + \frac{1 - 3w\Omega_{\text{de}}}{2} \frac{\partial D}{\partial \eta} - \frac{3}{2}\Omega_m[1 + \epsilon(k, \eta)]D = 0$$

scale-dependence of the linear modes

★ K-mouflage models:

$$\frac{d^2 D}{d\eta^2} + \left( \frac{1 - 3w_\varphi^{\text{eff}}\Omega_\varphi^{\text{eff}}}{2} + \epsilon_2 \right) \frac{dD}{d\eta} - \frac{3}{2}\Omega_m(1 + \epsilon_1)D = 0$$

Scale-independent modified linear growing mode

★  $f(R) : \epsilon(k, \eta) = \frac{k^2}{3(a^2 m^2 + k^2)}$

scalar field models:

$$\epsilon(k, \eta) = \frac{2\beta^2 k^2}{a^2 m^2 + k^2}$$

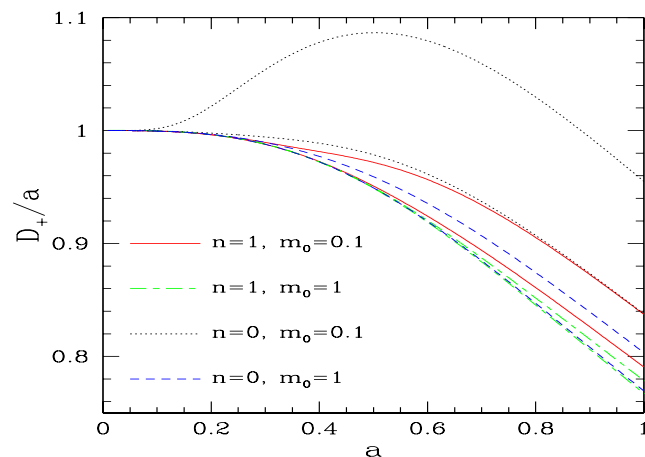


FIG. 1: Linear growing mode  $D_+(k, t)$  normalized to the scale factor  $a(t)$  for four  $(n, m_0)$  models. In each case we show the results for wavenumbers  $k = 1h\text{Mpc}^{-1}$  (lower curve) and  $k = 5h\text{Mpc}^{-1}$  (upper curve), as a function of  $a(t)$ . These two scales are in the non-linear regime and have only been chosen to exemplify the type of effects obtained in modified gravity.

Linear growing mode as  
a function of time

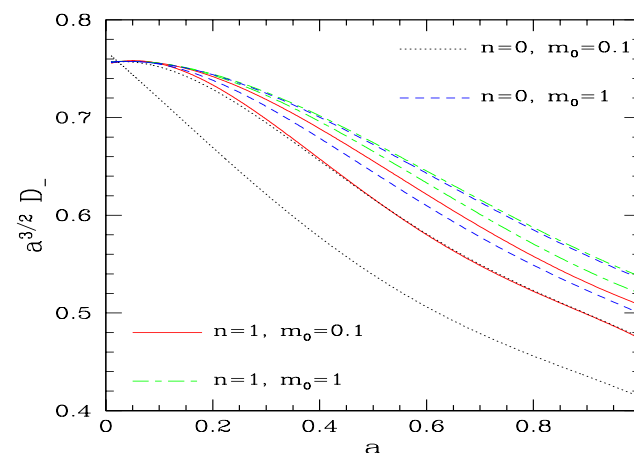


FIG. 2: Linear decaying mode  $D_-(k, t)$  normalized to  $a(t)^{-3/2}$  for four  $(n, m_0)$  models. In each case we show the results for wavenumbers  $k = 1h\text{Mpc}^{-1}$  (upper curve) and  $5h\text{Mpc}^{-1}$  (lower curve), as a function of  $a(t)$ . These two scales are in the non-linear regime and have only been chosen to exemplify the type of effects obtained in modified gravity.

Linear decaying mode as  
a function of time

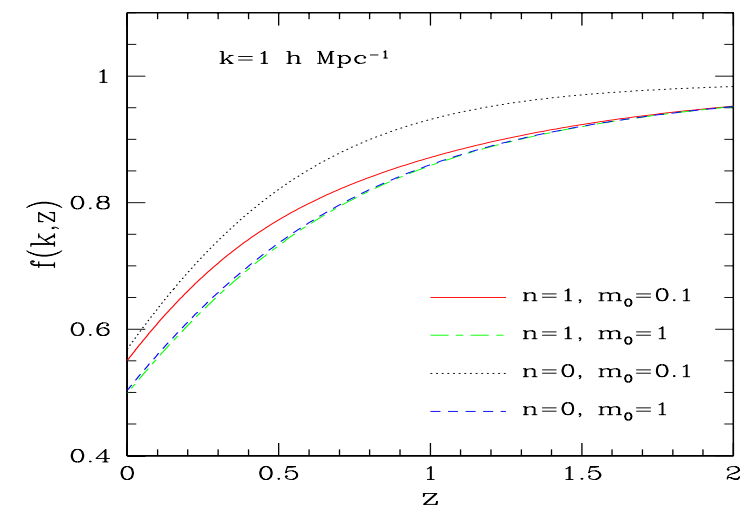


FIG. 5: Linear growth rate  $f(k, z) = \partial \ln D_+ / \partial \ln a$  for wavenumber  $k = 1h\text{Mpc}^{-1}$ , for four  $(n, m_0)$  models.

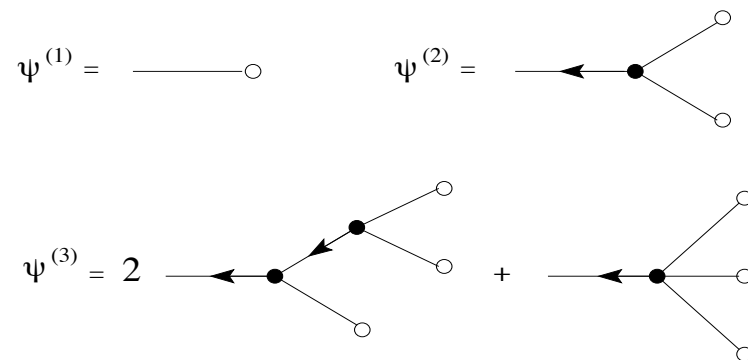
Linear growth rate as  
a function of time

## 6) One-loop power spectrum

As in the LCDM case, we can write the solution of the equation of motion as a **perturbative expansion** over powers of the linear growing mode:

$$\tilde{\psi}(x) = \sum_{n=1}^{\infty} \tilde{\psi}^{(n)}(x), \quad \text{with} \quad \tilde{\psi}^{(n)} \propto (\tilde{\psi}_L)^n$$

Diagrams:



- white circles: linear solution
- black dots: vertices
- lines with an arrow: retarded propagator

 new cubic vertex

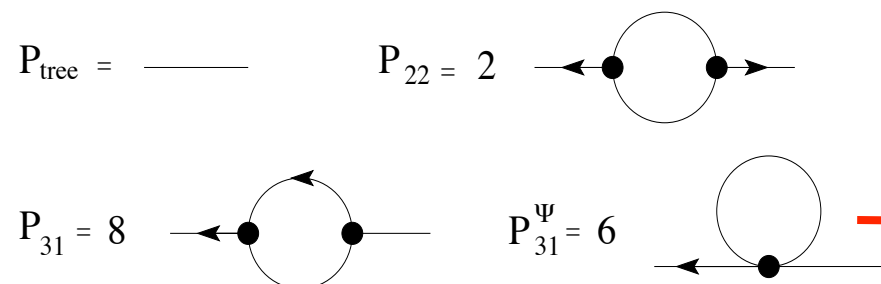
This gives in turns the density 2-pt correlation function, or the density power spectrum:

$$P(k) = P_{\text{tree}}(k) + P_{\text{1loop}}(k) + \dots$$

$$P_{\text{tree}} = P_L$$

$$P_{\text{1loop}} = P_{22} + P_{31} + P_{31}^{\Psi}$$

Diagrams:



 new diagram

In K-mouflage models, because there is no IR cutoff, the one-loop contribution to  $P(k)$  gives a (small) renormalization of the linear power spectrum:

$$P_{31}^{\Psi}(k) \sim P_L(k) \frac{\sigma_{sL}^2 a^2}{c^2 t^2} \frac{\kappa_2 \beta^4}{\kappa_1^4} \ll P_L(k)$$

## Relative deviations from LCDM for the power spectrum $P(k)$

### a) $f(R)$ models

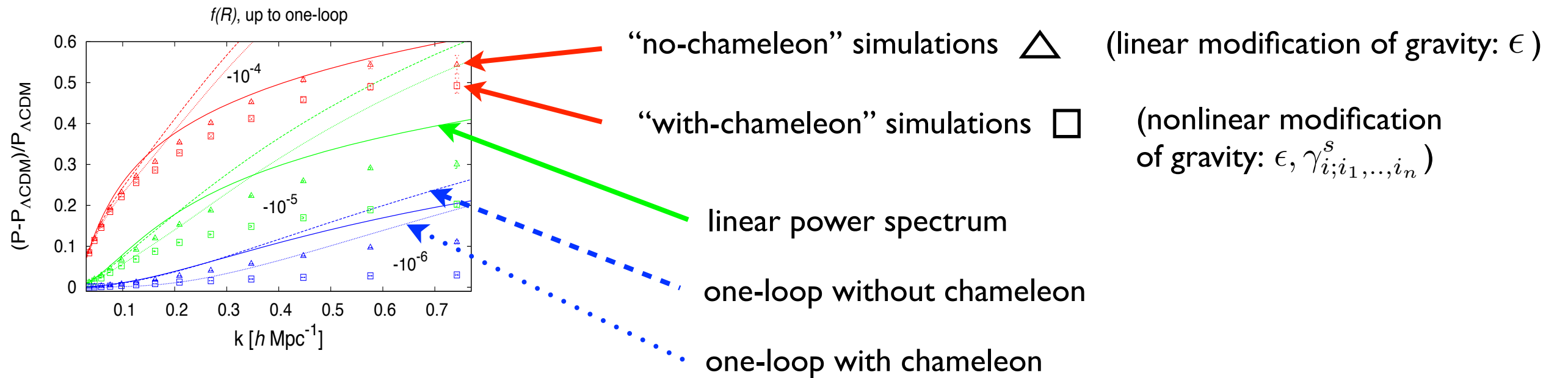
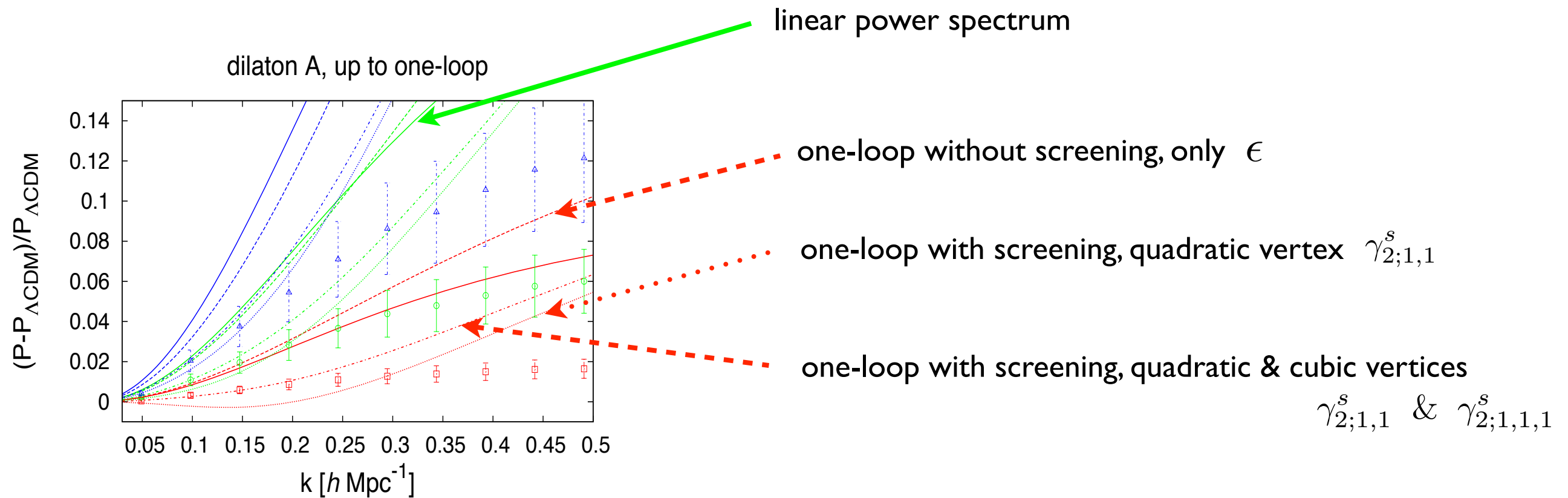


FIG. 3: Relative deviation from  $\Lambda$ -CDM of the power spectrum in  $f(R)$  theories, at redshift  $z = 0$ , for  $n = 1$  and  $f_{R0} = -10^{-4}, -10^{-5}$ , and  $-10^{-6}$ . In each case, the triangles and the squares are the results of the “no-chameleon” and “with-chameleon” simulations from [25], respectively. We plot the relative deviation of the linear power (solid line), of the one-loop power without “chameleon” effect ( $\gamma_{2;1,1}^s = \gamma_{2;1,1,1}^s = 0$ ) (dashed line), and with lowest-order “chameleon” effect ( $\gamma_{2;1,1}^s \neq 0, \gamma_{2;1,1,1}^s = 0$ ) (dotted line).

- ◆ Including the **quadratic vertex**  $\gamma_{2;1,1}^s$  gives the first sign of the **chameleon** effect.
- ◆ The cubic vertex makes no significant change.
- ◆ Going to 1-loop does not increase much the range of scales.

## b) Scalar field models

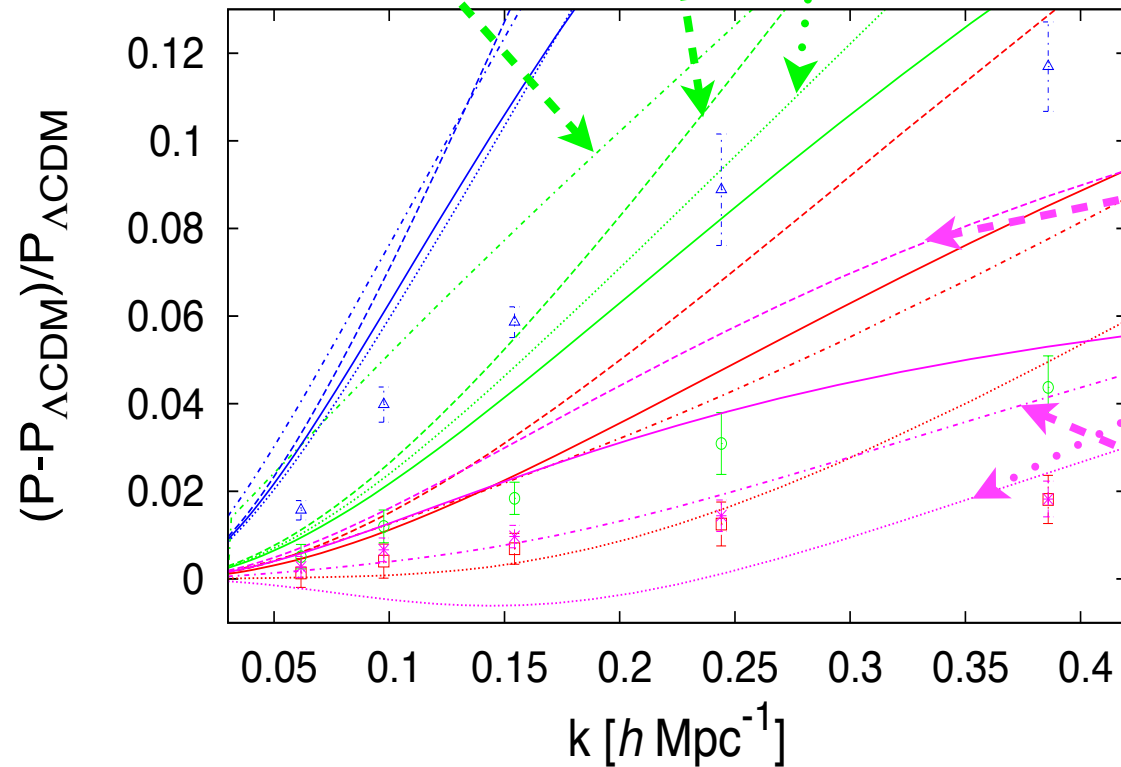


- ◆ Including the **quadratic vertex** gives the first sign of the **screening** effect.
  - ◆ This can “**over-correct**” the deviation from LCDM and give a power spectrum that is smaller than the LCDM one. (The linear term speeds up the collapse, but the quadratic term slows down and would halt the collapse before reaching high densities.)
  - ◆ The cubic vertex corrects for the “over-screening”.
- ➡ gradual **convergence** of higher orders on perturbative scales
- ◆ Going to 1-loop does increase somewhat the range of scales.

bad convergence

$\epsilon$  &  $\gamma_{2;1,1}^s$  &  $\gamma_{2;1,1,1}^s$        $\epsilon$        $\epsilon$  &  $\gamma_{2;1,1}^s$

symmetron A, up to one-loop



good convergence

$\epsilon$   
 $\epsilon$  &  $\gamma_{2;1,1}^s$   
 $\epsilon$  &  $\gamma_{2;1,1}^s$  &  $\gamma_{2;1,1,1}^s$

◆ For some models, going up to the cubic vertex can degrade the analytical predictions !

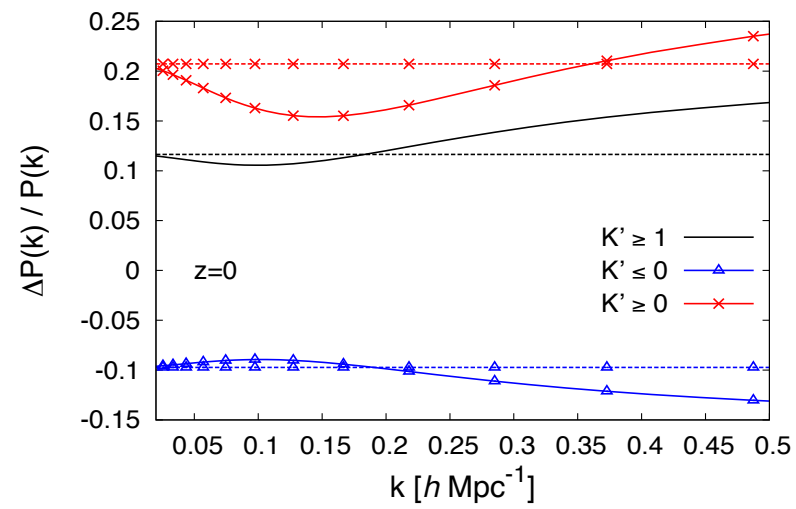
➡ bad convergence of higher orders

◆ This corresponds to models where the coupling functions are **singular**.

$$\beta(a) = \beta_0 \left[ 1 - \left( \frac{a_s}{a} \right)^3 \right]^{\hat{n}} \quad m(a) = m_0 \left[ 1 - \left( \frac{a_s}{a} \right)^3 \right]^{\hat{m}} \quad \hat{n} = 0.25, \quad \hat{m} = 0.5$$

### c) K-mouflage models

Scale-independent relative deviation in the linear regime.



relative deviation from LCDM for the linear (dashed line)  
and I-loop (solid line) power spectra



# Spherical collapse

To go **beyond** 1-loop standard **perturbation theory**, we wish to combine the perturbative expansion with a halo model.


take into account the impact of modified gravity on the halo mass function

 study how the spherical collapse is modified

5th force:  $\ddot{r} = -\frac{\partial \Psi_N}{\partial r} - \frac{\partial \Psi_A}{\partial r}$  (for f(R) and dilaton models)

normalized radius  $y(t)$ :  $y(t) = \frac{r(t)}{a(t)q}$  with  $q = \left(\frac{3M}{4\pi\bar{\rho}_0}\right)^{1/3}$ ,  $y(t=0) = 1$   $\delta(< r) = y^{-3} - 1$

$$\frac{\partial^2 y}{\partial \eta^2} + \frac{1 - 3w\Omega_{de}}{2} \frac{\partial y}{\partial \eta} + \frac{\Omega_m}{2} (y^{-3} - 1) y = \frac{-3\Omega_m y}{8\pi\mathcal{G}\bar{\rho}r} \frac{\partial \Psi_A}{\partial r}$$

 in GR, each shell evolve independently before shell crossing

 the 5th force depends on the profile

 all shells are coupled

Simplifying approximation: use an **ansatz for the density profile**, parameterized by the density contrast of the mass-shell of interest:

typical profile of rare events  
(neglecting nonlinear distortions)

$$\delta(x) = \frac{\delta_M}{\sigma_{x_M}^2} \int_{V_M} \frac{d\mathbf{x}'}{V_M} \xi_L(\mathbf{x}, \mathbf{x}')$$

## a) f(R) models

Normalized fluctuation of the Ricci scalar:


$$\delta R = 8\pi\mathcal{G}\bar{\rho}\alpha(x)$$

eq. of motion for the shell M:

$$\frac{d^2 y_M}{d\eta^2} + \frac{1 - 3w\Omega_{\text{de}}}{2} \frac{dy_M}{d\eta} + \frac{\Omega_m}{2} (y_M^{-3} - 1) y_M = \frac{-\Omega_m y_M}{2} \int_0^{x_M} \frac{dx x^2}{x_M^3} (\delta - \alpha)$$

constraint eq. for the new field:

$$\frac{d^2 \alpha}{dx^2} + \frac{2}{x} \frac{d\alpha}{dx} - \frac{(n+2)\Omega_{m0}}{\Omega_{m0}(1+\alpha) + 4\Omega_{\Lambda 0}a^{-3}} \left( \frac{d\alpha}{dx} \right)^2 = a^2 m_0^2 \left( \frac{\Omega_{m0}a^{-3}(1+\alpha) + 4\Omega_{\Lambda 0}}{\Omega_{m0} + 4\Omega_{\Lambda 0}} \right)^{n+2} (\alpha - \delta)$$

◆ Large scales: weak-field (linear) regime,  $\frac{d}{dx} \rightarrow 0, \quad \alpha \rightarrow \delta$   GR

◆ High density: strong-field (nonlinear) regime,  $\delta \rightarrow \infty, \quad \alpha \rightarrow \delta$   GR

 chameleon mechanism due to the nonlinearity.

Because of the 5th force, the **linear density threshold** to reach a given nonlinear density contrast (200) is **smaller** than for LCDM.

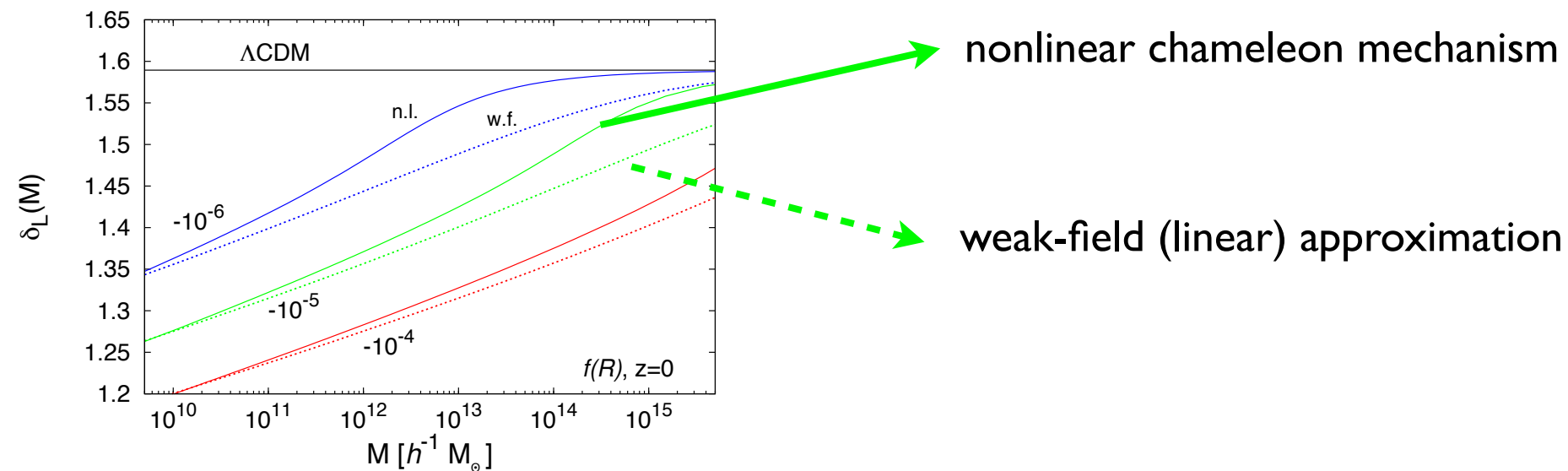


FIG. 6: Linear density threshold  $\delta_L(M)$ , associated with a nonlinear density contrast  $\delta = 200$ , for  $f(R)$  theories at  $z = 0$ . The dotted lines (w.f.) correspond to the weak-field limit (108) and the solid lines (n.l.) to the fully nonlinear constraint (106).

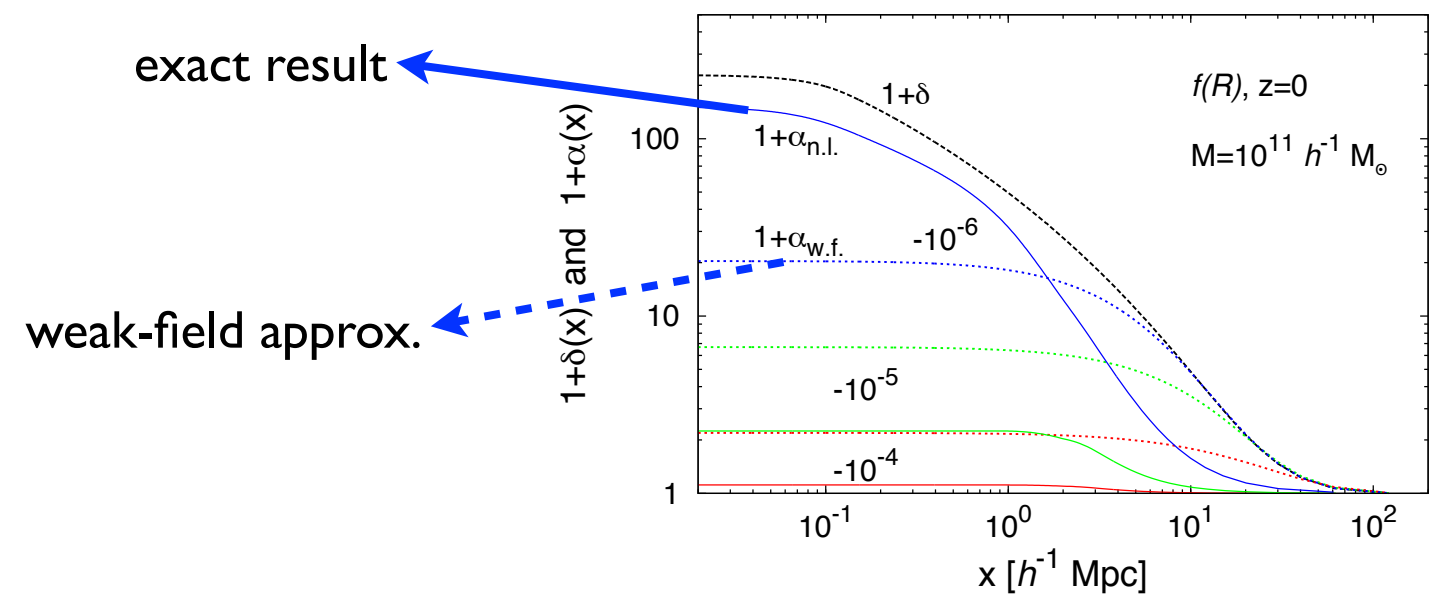
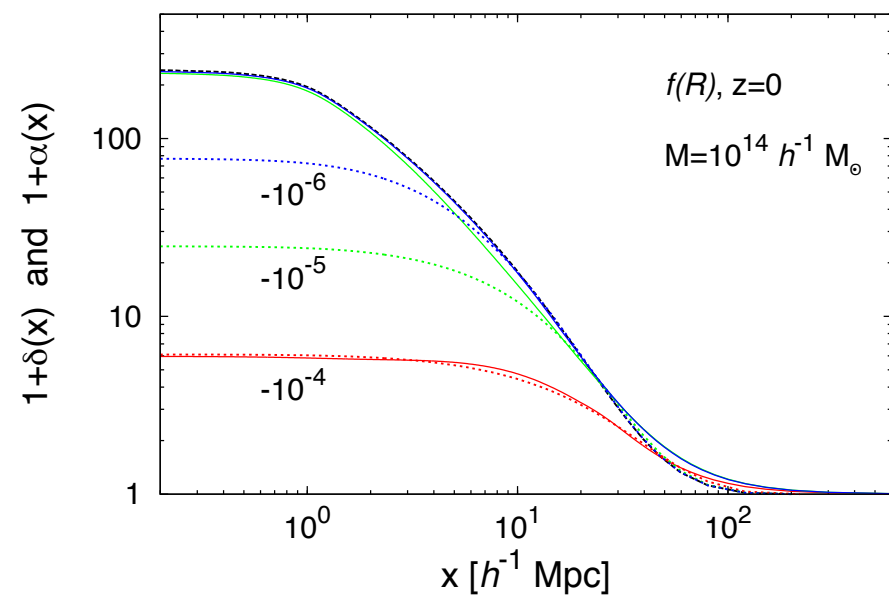
Chameleon effect is **greater for large masses**, where nonlinearities can overcome spatial gradients.

◆ The linear density threshold becomes **mass-dependent**:  $\delta_L(M)$

◆ The deviation from LCDM diminishes at high mass.

◆ The **nonlinear chameleon** effect decreases the deviation from LCDM. It is more efficient for large masses.

Nonlinear relaxation of the field  $\alpha(x)$  in high-density environments.




## b) Scalar field models

“Normalized” scalar field:  $\alpha(x) = a[\varphi(x)]$

eq. of motion for the shell M: 
$$\frac{d^2 y_M}{d\eta^2} + \frac{1 - 3w\Omega_{de}}{2} \frac{dy_M}{d\eta} + \frac{\Omega_m}{2} (y_M^{-3} - 1) y_M = \frac{-9\Omega_m a \beta_\alpha^2 y_M}{m_\alpha^2 \alpha^4 x_M} \frac{\partial \alpha}{\partial x}$$

Klein-Gordon eq.: 
$$\frac{d^2 \alpha}{dx^2} + \frac{2}{x} \frac{d\alpha}{dx} + \left[ \frac{d \ln \beta_\alpha}{d\alpha} - 2 \frac{d \ln m_\alpha}{d\alpha} - \frac{4}{\alpha} \right] \left( \frac{d\alpha}{dx} \right)^2 = \frac{m_\alpha^2 \alpha^4}{3a} \left[ 1 + \delta - \frac{a^3}{\alpha^3} \right]$$

◆ Large scales: weak-field (linear) regime,  $\frac{d}{dx} \rightarrow 0$ ,  $\alpha \rightarrow a(1 + \delta)^{-1/3}$   GR

◆ High density: strong-field (nonlinear) regime,  $\delta \rightarrow \infty$ ,  $\alpha \rightarrow a\delta^{-1/3}$

dilaton models:  $\frac{\beta_\alpha^2}{m_\alpha^2} \rightarrow 0$

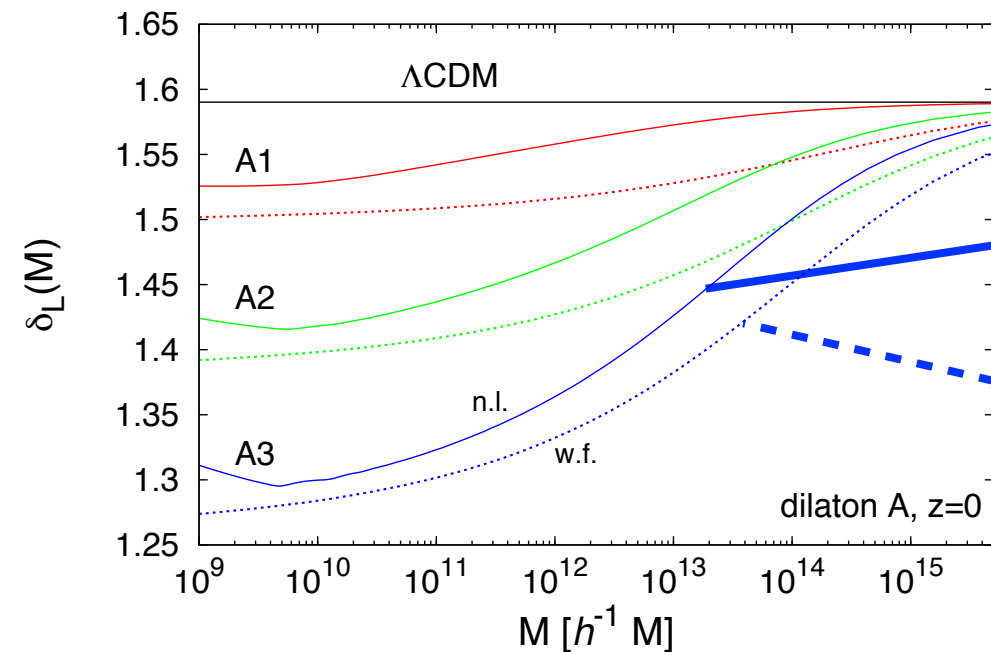
symmetron models:  $\alpha \rightarrow a_s$

 GR

 screening mechanism due to the nonlinearity.

Because of the 5th force, the **linear density threshold** to reach a given nonlinear density contrast (200) is **smaller** than for  $\Lambda$ CDM.

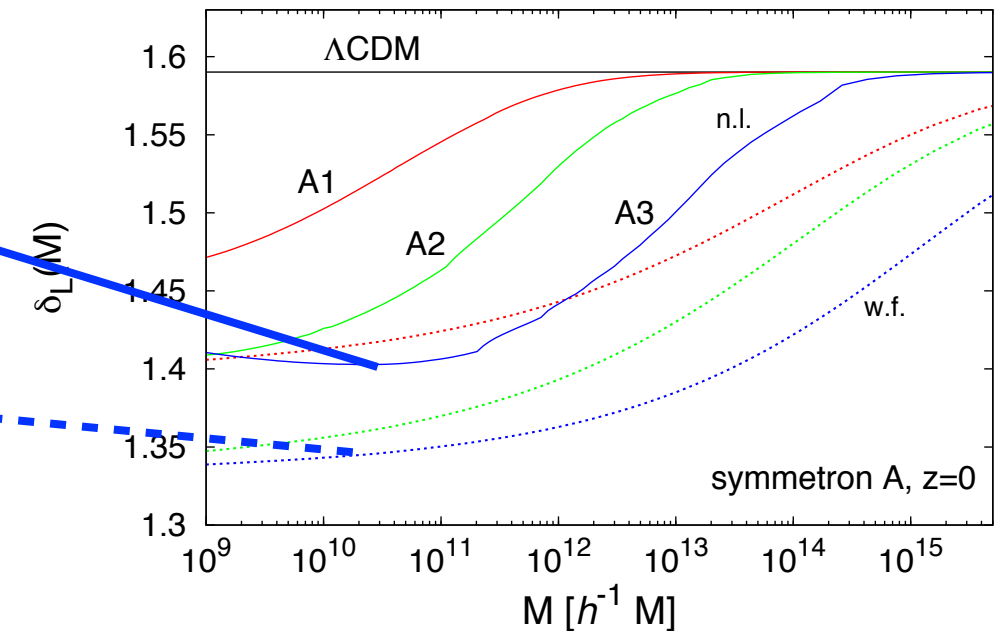
### dilaton models



nonlinear  
screening

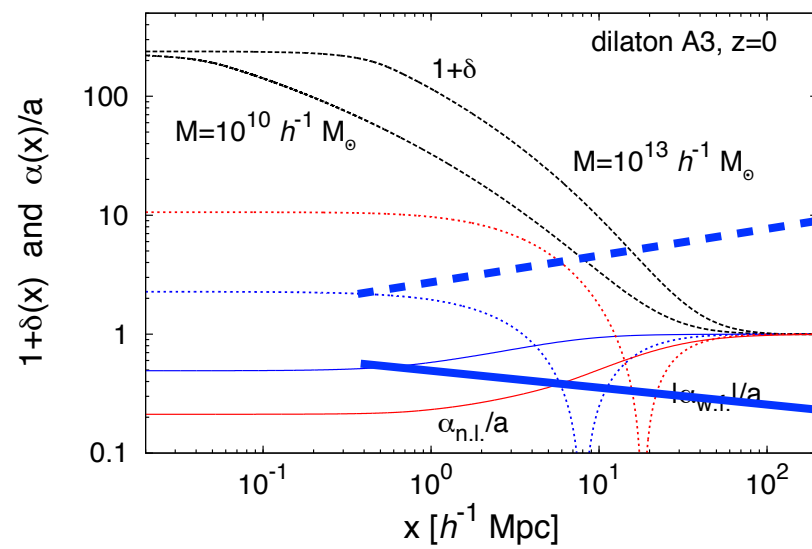
weak-field approx.

### symmetron models



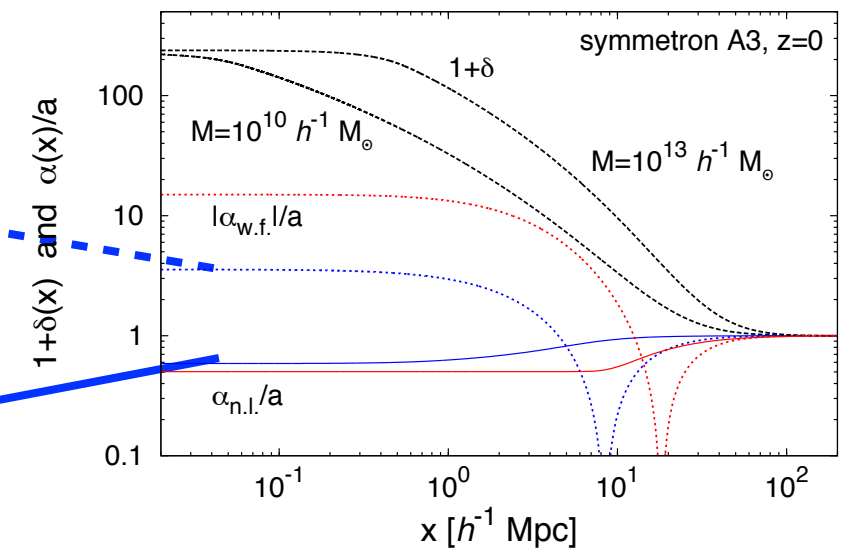
- ◆ Again, nonlinearities (screening) decrease the deviation from GR.
- ◆ The rate of convergence to GR at high mass depends on the model (very efficient for symmetron, very nonlinear models).
- ◆ Contrary to  $f(R)$  models, at low mass we do not converge to weak-field prediction but to GR.

Nonlinear relaxation of the field  $\alpha(x)$  in high-density environments.



weak-field approx.

exact result



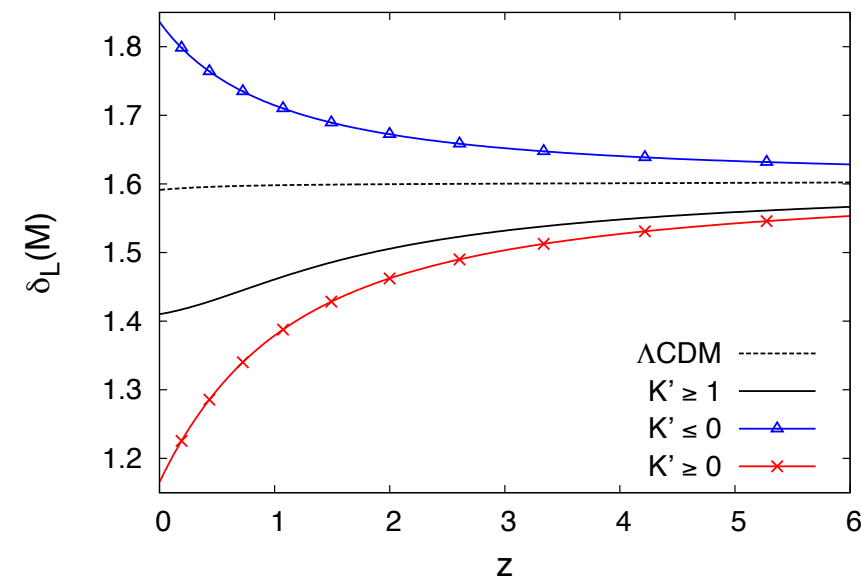


### c) K-mouflage models

Trajectories in physical coordinates: 
$$\ddot{\mathbf{r}} + \frac{d \ln \bar{A}}{dt} \dot{\mathbf{r}} - \left( \frac{\ddot{a}}{a} + \frac{\dot{a}}{a} \frac{d \ln \bar{A}}{dt} \right) \mathbf{r} = -\nabla_r (\Psi_N + \ln A)$$

Scale-independence  $\rightarrow$  the motions of different mass shells are decoupled, as in LCDM (before shell-crossing)

linear density contrast threshold:



Depending on the sign of  $K'$ , structure formation proceeds faster or slower than in LCDM.

Departure from LCDM grows faster at low  $z$  for models where  $\bar{K}' \rightarrow 0$

# Matter power spectrum

Use a halo model:

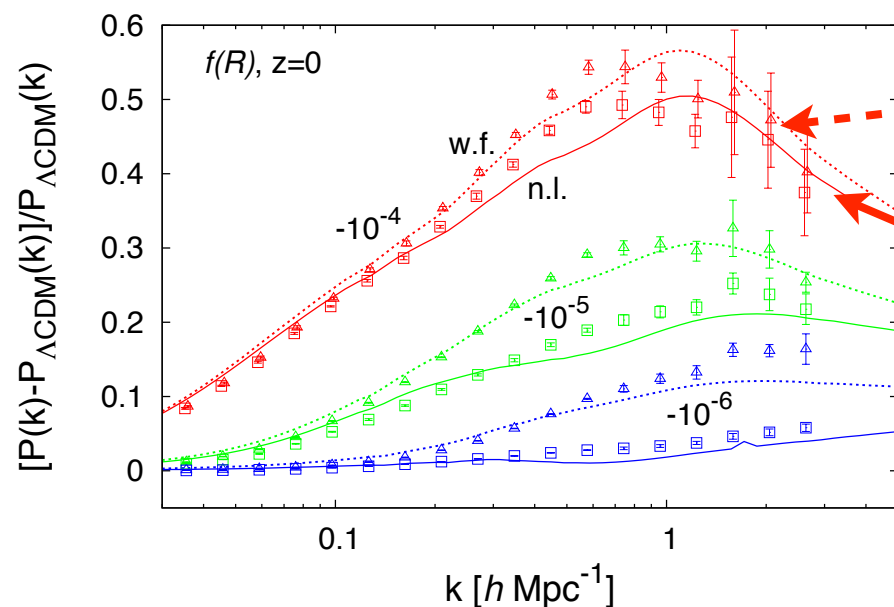
$$P(k) = P_{1H}(k) + P_{2H}(k)$$

halo mass function  
halo density profile

perturbation theory  
Lagrangian-space interpretation  
adhesion-like regularization

## a) $f(R)$ models

Relative deviation from  $\Lambda$ CDM for  $P(k)$



“no-chameleon” simulations  $\triangle$  (linear modification of gravity:  $\epsilon$ )

“with-chameleon” simulations  $\square$  (nonlinear modification of gravity:  $\epsilon, \gamma_{i;i_1,\dots,i_n}^s$ )

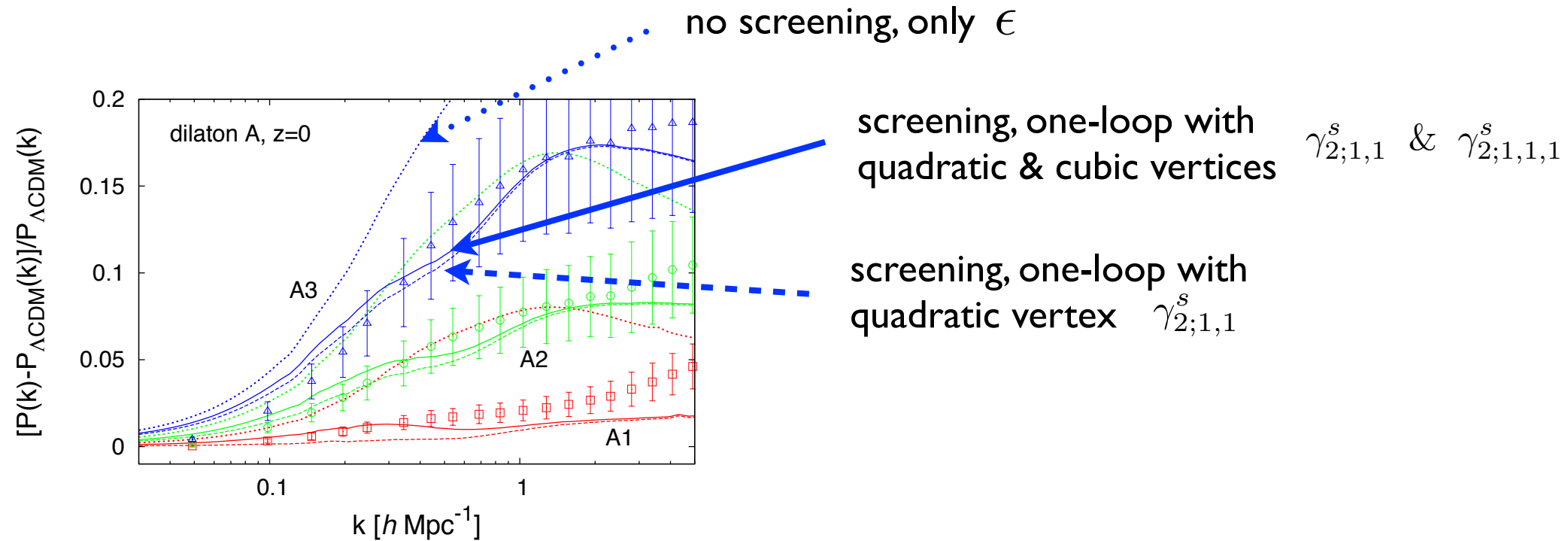
FIG. 13: Relative deviation from  $\Lambda$ -CDM of the power spectrum in  $f(R)$  theories, at redshift  $z = 0$ , for  $n = 1$  and  $f_{R_0} = -10^{-4}, -10^{-5}$ , and  $-10^{-6}$ . In each case, the triangles and the squares are the results of the “no-chameleon” and “with-chameleon” simulations from [25], respectively. We plot the relative deviation of the nonlinear power spectrum without chameleon effect (w.f., dotted lines) and with chameleon effect (n.l., solid lines).

◆ **Reasonably good agreement** between simulations and analytical predictions, from linear to mildly nonlinear scales.

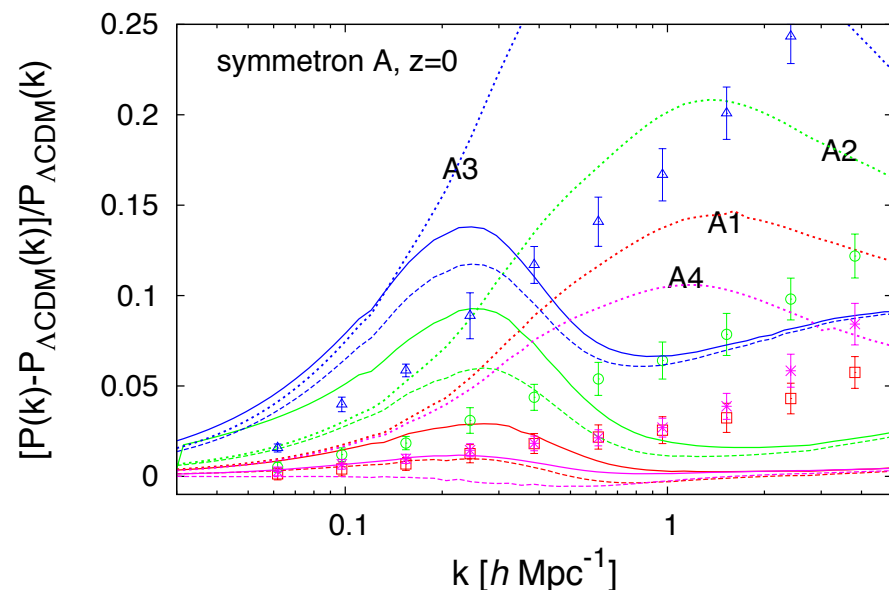
◆ As compared with parameterizations (PPF), the convergence to GR on small scales is **not put by hand**. It is due to the chameleon mechanism.

## b) Scalar field models

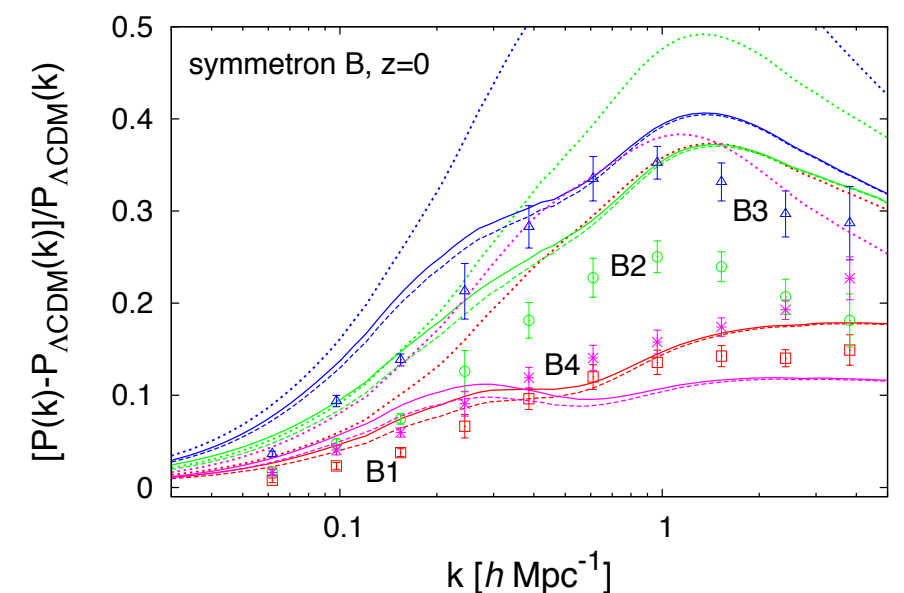
Relative deviation from  $\Lambda$ CDM for  $P(k)$



- ◆ The impact of the nonlinear screening mechanism is greater than for the  $f(R)$  models.
- ◆ Reasonably good agreement with simulations.
- ◆ Underestimate at high  $k$ , could be due to the neglect of halo profile modifications.



Bad convergence, but we can guess beforehand the problematic cases.



Good convergence, reasonable agreement.

## c) Origin of the deviation from LCDM

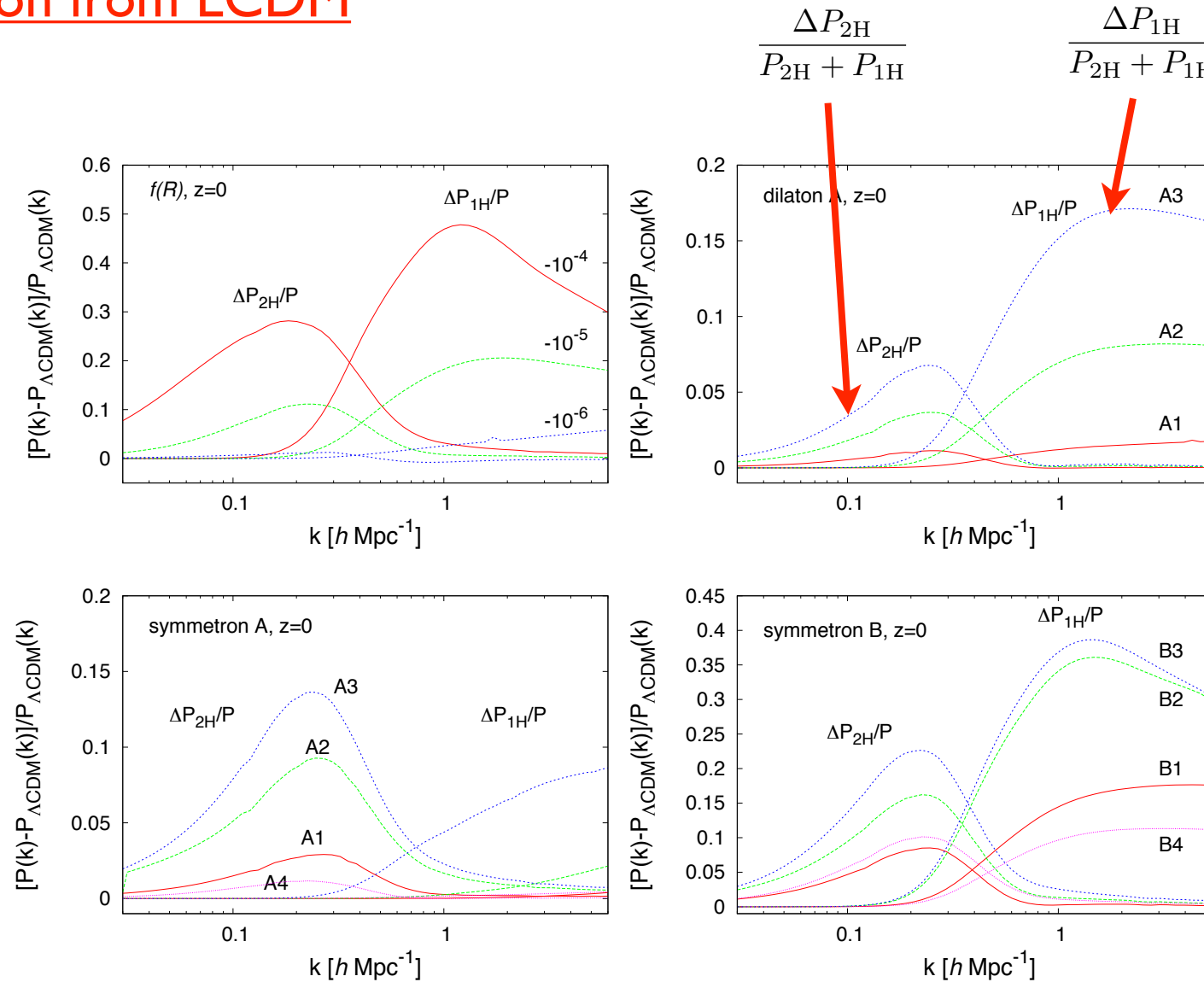
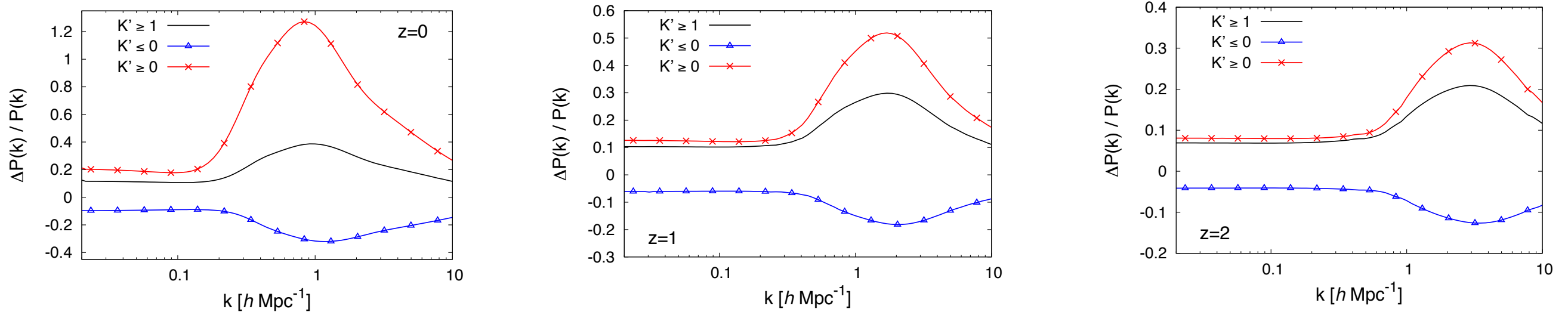


FIG. 16: Relative deviation from  $\Lambda$ -CDM of the power spectrum in  $f(R)$ , dilaton, and symmetron models, at redshift  $z = 0$ . For each model, we show the contribution from the modification to the two-halo term,  $\Delta P_{2H}/(P_{2H} + P_{1H})$  (curves with a peak around  $k \sim 0.2 h \text{ Mpc}^{-1}$ ), and the contribution from the modification to the one-halo term,  $\Delta P_{1H}/(P_{2H} + P_{1H})$  (curves with a peak around  $k \sim 2 h \text{ Mpc}^{-1}$  or which keep growing at high  $k$ ). We only consider the results with the full chameleon or screening effects.

- ◆ At low  $k$ , impact from the 2-halo term (perturbation theory).
- ◆ At high  $k$ , impact from the 1-halo term (spherical collapse).
- ◆ Need to go beyond linear theory, and even beyond the perturbative regime.

## d) K-mouflage models



relative deviation from  $\Lambda$ CDM of  $P(k)$ , at  $z=0, 1, 2$ .

At low  $k$  we recover the linear and 1-loop results.

The deviations are amplified on mildly nonlinear scales:

- later stages of the dynamics
- large-mass tail of the halo mass function

The deviations decrease at high  $k$ : low-mass tail and inner halo regions

The sign of the deviation depends on the sign of  $K'$

The relative deviations are significantly greater ( $\sim 10$ ) than for background quantities such as  $H(z)$ . One can keep a background very close to  $\Lambda$ CDM while obtaining 10% deviations for matter clustering.

The deviations from  $\Lambda$ CDM decrease rather slowly at higher  $z$

# Conclusion

- ◆ “Modified-gravity” models introduce a **new degree of freedom** (new field).
- ◆ Using the **quasi-static approximation**, we can go back to the standard framework, defined by the matter density and velocity fields, with a modified “gravitational” potential.
  - ◆ “Standard” perturbation theory can be generalized in a direct manner.  
The main differences are:
    - new complex **time** and **scale dependences**.
    - new **nonlinear vertices** (the eqs. of motion are no longer quadratic), which are the first signs of nonlinear screening mechanisms.
- ◆ The spherical collapse is more complex, because of the **coupling between different shells**. Nevertheless, this can be simplified using approximate density profiles.
  - ◆ Explicit account of **nonlinear chameleon or screening** mechanisms that ensure convergence to GR in high-density environments.
- ◆ By combining perturbation theory and halo model (spherical collapse), one can obtain **reasonably good predictions** up to mildly nonlinear scales, for models that are not too singular.
- ◆ **Singular** models lead to **bad convergence** of perturbative expansions and low accuracy of analytical predictions. Fortunately, these cases can be detected before hand.
- ◆ To handle difficult cases, or to go beyond the quasi-static approximation, one may need to explicitly keep track of the new scalar field in the perturbative approach ?

## Problems:

- beyond the quasi-static approximation
- cases where the perturbative expansion over the scalar field is not well behaved
- halo profiles (mass-concentration relation)
- taking into account neutrinos/baryons
- bias



Thank you

